Journal of Mechanical Engineering Research and Developments
ISSN: 1024-1752
CODEN: JERDFO
Vol. 43, No. 1, pp. 342-350
Published Year 2020

Study On Behavior And Breakup Process Of Oil Jet Ejected From Curved Pipe

G. Nitta†, A. Nakashima‡, K. Mimura†, K. Nishida†, H. Hongou‡, H. Yokohata‡ & Y. Ogata†

†Department of Mechanical Engineering, Hiroshima University Kagamiyama 1-4-1, Higashi-Hiroshima, Hiroshima 739-0041, Japan
‡Mazda Motor Corporation Shinchi 3-1, Fuchu-cho, Aki-gun, Hiroshima 730-8670, Japan
*Corresponding Author Email: m182486@hiroshima-u.ac.jp

ABSTRACT: This research focuses on oil jet behaviour ejected from 90-degree bend pipe and flow distribution inside the pipe for jet Reynolds number *Re* (*Re* = $W_m d/v$ where W_m: oil jet mean velocity, *d*: nozzle diameter, *v*: kinematic viscosity) from 1500 to 3000. The high-speed camera is used to observe the oil jet from four side views with 20,000 fps. It is found that higher *Re* leads wider position and higher standard deviation of oil jet interface. Jet interface begins to fluctuate close to the nozzle tip with increasing *Re*. Droplets are generated from jet interface and ligaments above *Re*=2500, and the number of droplets increases with increasing *Re*. The 50% of total droplets are generated and droplets diameter around 300μm is mostly observed in the inner side of the pipe bend. In *Re*=3000, a lot of ligaments and a few bags appear, and droplets produced from bags are smaller than from ligaments. Stereo PIV (Particle Image Velocimetry) technique is used to observe the secondary flow in the nozzle. It is found that the mainstream flow velocity of outer side is faster than of inner side in all Reynolds numbers. Though the Dean vortex is observed at *Re*=1500, flow from the outer side to the inner side begins to appear and flow from inner to outer side impinges each other at the center of the nozzle at *Re*=2000, and flow from inner to outer side disappeared and Dean vortex is reversed at *Re*=2500 in our experiments. The secondary flow above *Re*=2500 is regarded as the 50% of total droplets at the inner side of the bend.

INTRODUCTION

High compression ratio makes it possible to increase thermal efficiency of automotive engines in general, but the high compression ratio leads high thermal loading of the piston. Therefore, the piston should be cooled efficiently not to be damaged because it is one of the most important components in the engine. There are two ways to reduce the piston temperature using engine oil, oil jet impingement on underside of the piston wall and inflow of the jet into a piston cooling gallery [1-4]. The oil jet impingement method is commonly used in gasoline and diesel engines for a few decades. The cooling gallery method is installed in recent year especially in the diesel engine. To control the impingement behavior at the piston underside and the oil inflow efficiency into the gallery, it is important to determine the optimum oil jet flow and jet shape. Although the cooling performance increases in high flow rate of engine oil, more oil mist which causes the oil consumption because of oil combustion is generated in higher flow rate. It is therefore important to develop cooling technologies that are still capable of sufficient heat transfer at the piston wall by low oil jet flow rates.

Generally, the oil is ejected from the curved nozzle which is set on the crankcase. A flow field in the jet results in a complex velocity distribution compared to the flow field ejected from straight pipe due to the secondary flow. Previous studies mainly focused on the liquid jet ejected from the straight pipe and the gas jet ejected from the curved pipe. Sudo measured the gas jet velocity distribution ejected from the curved pipe at Reynolds number of *Re*=40000 and they found that the flow field after the 10D (D: nozzle diameter) is affected by the flow distribution at the nozzle exit [5-6]. Arai and Amagai measured interfacial fluctuation of the water jet ejected from straight pipe with the photoelectric sensor [7]. Gong measured wave length and frequency on the liquid jet with a high speed camera. According to their results, the wave on the jet is classified in four types [8-9]. There are only a few studies which clarify the phenomena of the high viscosity jet compared to water ejected from the curved pipe.

In this research, we measured the oil jet width, interfacial fluctuation, droplets diameter produced from the jet interface to clarify the effects of curved pipe and jet Reynolds number. In addition, we conducted the experiment in which we measure the nozzle internal flow velocity distribution after bend with the stereo PIV method.

EXPERIMENTAL SETUP

We conduct the two types of experiments, one is visualization experiment to observe the oil jet fluctuation, another is the stereo PIV to measure the flow velocity distribution in a cross section of the nozzle. Fig. 1 shows the geometry of 90-degree bend nozzle. The nozzle diameter (d) is 6mm and the length after the bend (L) is 30mm. It is made of transparent acrylic for measuring the flow velocity inside the nozzle with the PIV. The curved pipe with a single bend is used to clarify effects of pipe bend on flow field in the pipe and behavior of jet ejected from the nozzle. The coordinate used here is defined as Fig. 2. To understand the direction easily, Front (Fr), Rear (Rr), Inner (In) and Outer (Out) are also defined. The transparent silicone oil (KF-56A, Shin-etsu chemical) is used instead of engine oil because the stereo PIV requires the transparent liquid to measure the flow velocity distributions. The refractive index of silicone oil is well matched with acrylic of which the nozzle is made. The kinetic viscosity, the specific gravity and the refractive index of silicon oil are 15mm^2/s, 0.995 and 1.498 of the transparent oil respectively. The surface tension and kinetic viscosity of this oil are close to that of 80℃ engine oil (SAE 0W30).

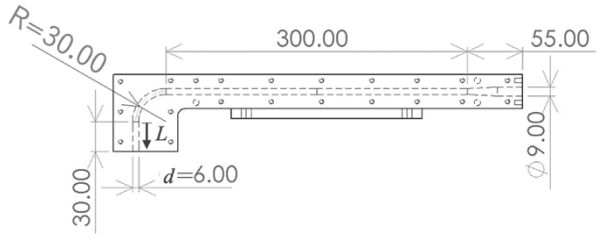

Figure 1. The size of nozzle for visualization experiment

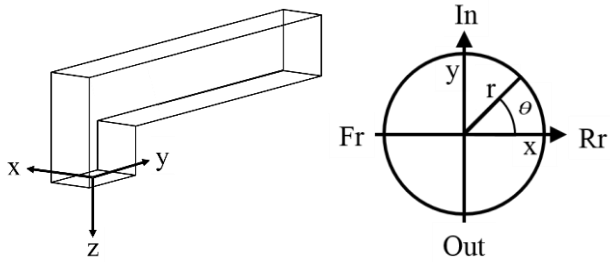

Figure 2. The definition of the coordinate system

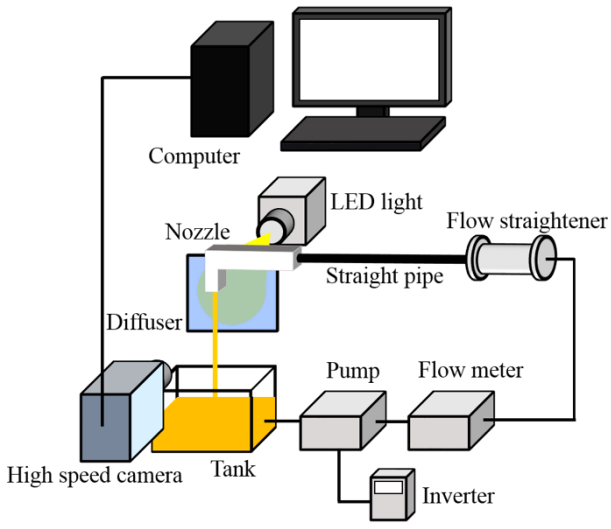

Figure 3. Experimental apparatus for visualization experiment

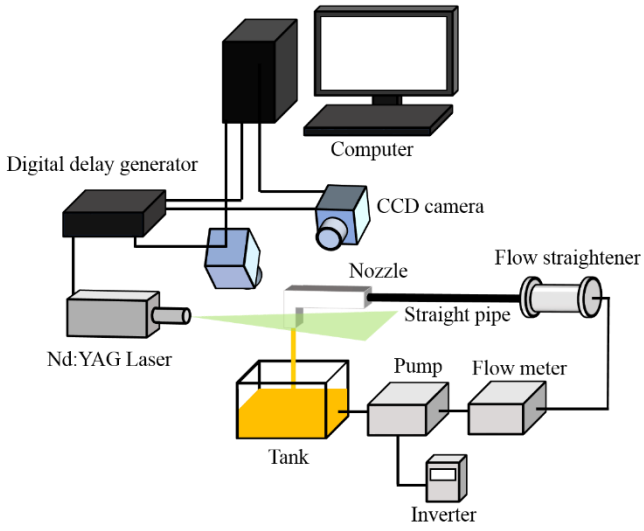

Figure 4. Experimental apparatus for stereo PIV experiment

Table 1. The experimental conditions

	Stereo PIV	Visualization
Camera	CCD Cameras	High Speed Camera
Oil	Silicon Oil	
Re number	1500, 2000, 2500	1500, 2000, 2500, 3000
Ambient temperature	298 ± 3 K	
Oil temperature	298 ± 1.5 K	
Measurement period	15 sec (20 Hz)	1 sec (20,000 Hz)
Measurement sections	$L/d = 4.5$	$z/d = 0$ to 25

Fig. 3 shows the schematic experimental apparatus for oil jet visualization. To observe the oil jet behavior, we took the image with the high speed camera (SA-Z, Photron) and the LED light (LLBK1-LA-W-0001, AITEC SYSTEM) as a back light. The flow straightener and 1500mm straight pipe were installed to rectify the flow before the oil entered the nozzle. The inverter can adjust the flow rate by the pump rotation speed. The section size for oil jet visualization was 150mm along the jet axis. The shape of oil jet interface was captured by photographing in the range of 50mm at the jet direction, thus jet interface was photographed at three different positions by positioning the camera per 50 mm intervals. The images were analyzed using the FtrPIV software (Flowtech Research) to count the number and to measure diameter of droplets.

Fig. 4 shows the schematic experimental apparatus for stereo PIV. The oil circulation system was the same as Fig. 3, but the optical system was different from Fig. 3. Two CCD cameras were set in stereo position and image size taken by the cameras was 1200×1600 pixels. Fluorescent tracer particles (Fluostar0459, average particle size: 15μm, EBM Corporation) that were mixed in the oil were excited by Nd:YAG LASER of 532nm, and the particles emitted light at 580nm. To synchronize the camera and the LASER, the digital delay generator (VSD2000, Flowtech Research) was connected. Velocity fields obtained via PIV were also analyzed using FtrPIV. Table 1 summarizes the experimental conditions of visualization experiment of oil jet behavior and nozzle internal flow velocity measurement. The nozzle internal flow distribution is measured at the L/d=0.5 upstream from the nozzle exit. The Reynolds number based on quantity of the nozzle tip can be calculated by where the area-averaged streamwise velocity at the nozzle exit is $W_m = 4Q/\pi d^2$ (Q: flow rate, d: nozzle diameter).

$$Re = \frac{W_m d}{\nu}$$

In this research, the profiles of the oil jet interface were acquired by image processing. First, the original images were converted to the grayscale images. Next, the binarization was performed with the Otsu method [10] to determine the oil jet interface. At last, the interfacial position of only oil jet is acquired by removing the satellite droplets and filling voids in the liquid column.

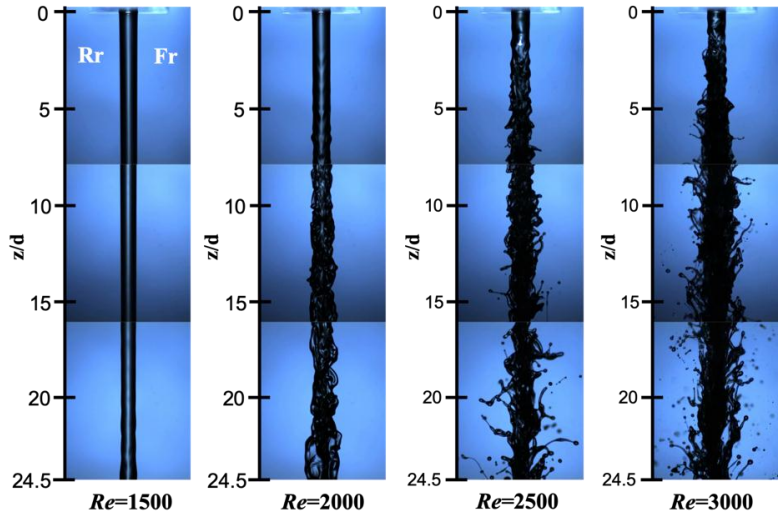

(a) In-side and Out-side

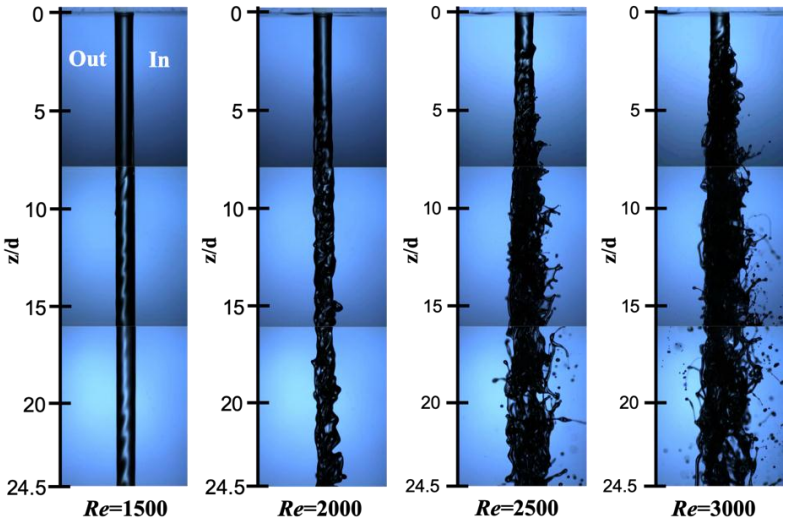

(b) Fr-side and Rr-side.

Figure 5. The effect of Re on jet behavior. (a) In-side and Out-side (b) Fr-side and Rr-side.

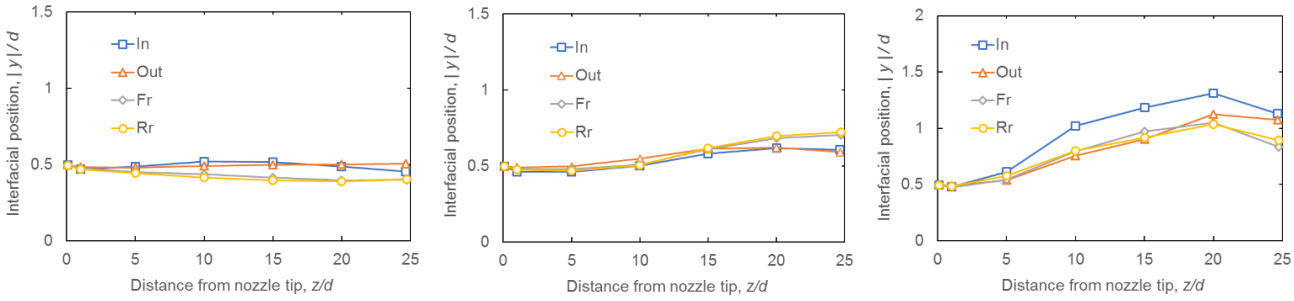

Figure 6. Interfacial position of each sides at *Re*=1500(left), 2000(center), 2500(right)

[Reproduced from Ref. [11]]

RESULTS AND DISCUSSION

Visualization of oil jet behavior

Fig. 5 (a) and (b) shows the photographic images of the In-side and Out-side and Fr-side and Rr-side oil jet behavior from z/d = 0 to 24.5 within Re range of 1500 to 3000, respectively. The images were taken at the three different areas from z/d = 0 to 7.8, from 7.8 to 15.9 and 15.9 to 24.5 to observe the steady oil jet with high resolution. Therefore, three images that were not taken at the same time are connected to show the whole behavior of steady jets. Using the back-light illumination, the black area shows the oil jet and blue area shows the background.

The oil jet interface in low *Re* number conditions were smooth and the droplets were not generated from oil interface in the observation sections below *Re*=2500. Especially in the condition of *Re*=1500, the wave on the interface does not exist in the observation sections. Above *Re*=2000 conditions, the oil jet interface begins to fluctuate, and fluctuation becomes more intense with increasing of *Re* number. The waves on the oil jet interface glow and some of wave crests become ligaments. When *Re* is 2500 or more, droplets are generated from the ligaments. As Fig. 5 (a) shows, the In-side interface fluctuates on a larger scale, and the numbers of droplets and ligaments are larger than the other three sides. The wave velocity of In-side is faster than Out-side. As Fig. 5 displays the number of droplets and ligaments, the interfacial fluctuation and the wave velocity are approximately the same between Fr-side and Rr-side.

Fig. 6 plots the results of the interfacial position divided by nozzle diameter, $|y|/d$, as a function of *Re* at various z/d values. The interfacial position was acquired by image processing as written in experimental setup section. The interfacial position in *Re*=1500 is almost constant from nozzle tip to the end of the measuring section at any side. In *Re*=2000, the interfacial position begins to increase at z/d= 10 and the jet widths of Fr-side and Rr-side are wider than In-side and Out-side after z/d = 15. The jet interface begins to fluctuate close to the nozzle tip for high Re numbers. In *Re*=2500, the position at which fluctuation begins is z/d=5 and the interfacial position of In-side is the widest at any measuring point below z/d = 5. The interfacial position decreases from z/d=20 to 25 in *Re*=2500 because the degree of breakup which formed droplets increased going downstream. These results demonstrate that with increasing *Re* number, the jet width increases and the position at which the fluctuation begins is closer to nozzle tip.

Measurement of the Curved Nozzle Internal Flow

To investigate the effect of the curved nozzle, the internal flow in the pipe is discussed. The stereo PIV method was used to measure the 2D3C velocity distributions inside the nozzle cross-sections. Fig. 7 shows streamwise velocity distributions and secondary flows by color contours and vectors, respectively, based on the averages of 300 pairs at *Re*=1500, 2000 and 2500.

At *Re*=1500, the flow from In-side to Out-side is dominant at the center of the nozzle and the Dean vortex is formed. The flow from the Out-side to the In-side begins to appear and another flow from In-side to Out-side impinge to the flows each other at the center of the nozzle at *Re*=2000. At *Re*=2500, flow from In-side to Out-side disappears while flow from Out-side to In-side still remains, which causes the reversed Dean vortex. The axial velocity is high on the Out-side and low on the In-side in all *Re* numbers because of the centrifugal force. However, the velocity distributions are a little bit different at every *Re* numbers. The axial velocity distributions are strongly affected by the secondary flow. At *Re*=1500, the high velocity area is in the Out-side and it spreads out to Fr-side and Rr-side. On the other hand, the high velocity area is spreads out to the center at *Re*=2000 and 2500.

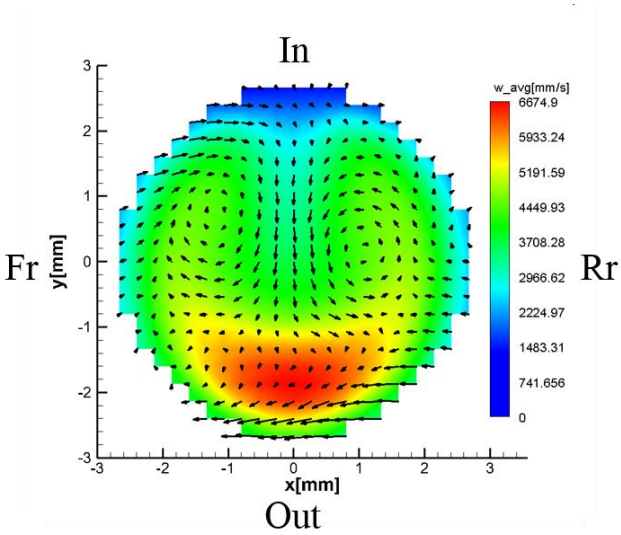

(a) Flow distribution at L/d=5 at Re=1500

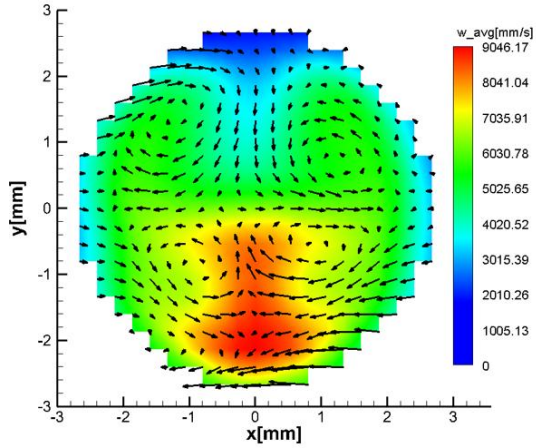

(b) Flow distribution at *L/d*=5 at *Re*=2000

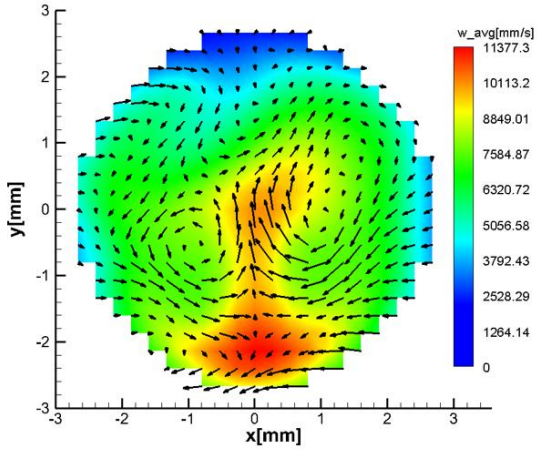

(c) Flow distribution at *L/d*= 5 at *Re*=2500

Figure 7. The flow distribution at *L/d*=5 at *Re*=1500 (a), 2000 (b), 2500 (c). Arrow indicate in-plane velocity components and contours indicate the streamwise velocity distributions.

From these results, it is considered that nozzle internal flow affects the oil jet behavior. At *Re*=2000, the oil jet width of Fr-side and Rr-side is wider than of In-side and Out-side, because the secondary flow inside the nozzle formed the flow from center to Fr-side and Rr-side. Additionally, at *Re*=2500, the flow from Out-side to In-side is dominant along the cross-section and it is considered that flow made the interfacial position in In-side spread out.

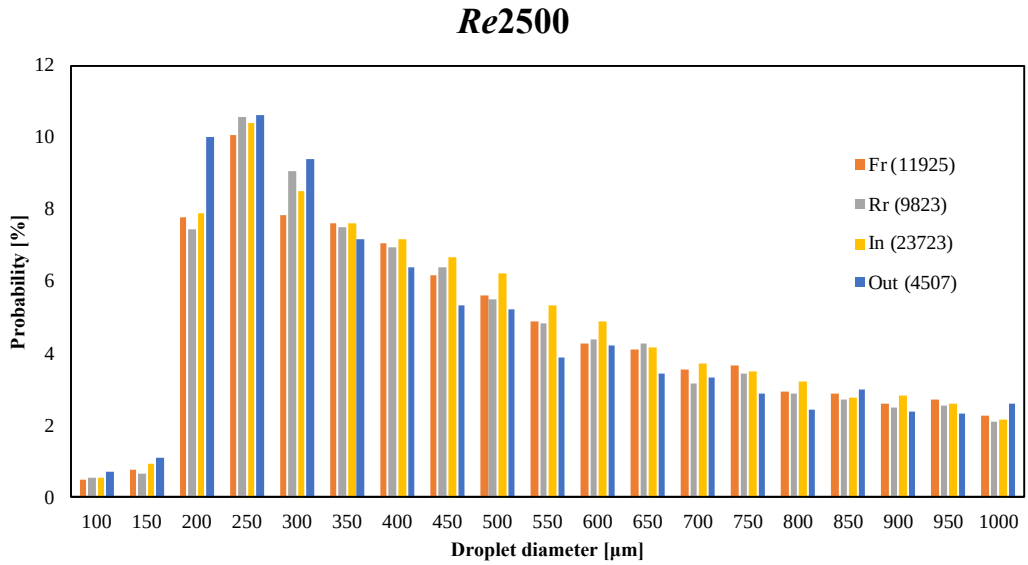

(a) The droplet diameter distribution at Re=2500

(The total number of detected droplets is 49,978)

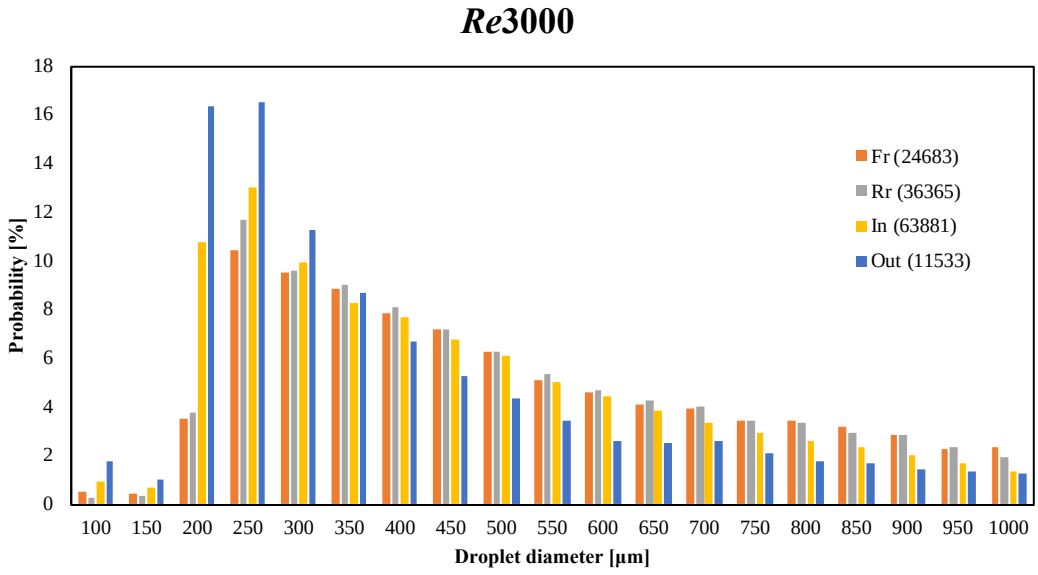

(b) The droplet diameter distribution at *Re*=3000

(The total number of detected droplets is 136,462)

Figure 8. The droplet diameter distribution. (a)Re=2500, (b)Re=3000

The droplet diameter

At *Re*=2500 and 3000, the droplets generation from the jet interface was observed in four sides. The results of droplet diameter histogram at both *Re* numbers are shown in Fig. 8. The histograms show the probability as function of the droplet diameter from 100μm to 1000μm per 50μm. The droplets were detected from the images which were selected with time interval of 50ms. The time interval is enough not to detect the same droplets twice. The total number of droplets at each side is shown in the legend.

At both *Re* numbers, the number of droplets at In-side was the most and the number of droplets at Out-side was the least. Approximately the half of droplets was detected in the In-side and 40% of droplets was detected in the Fr-side and Rr-side. The total number of droplets in each side at *Re*=3000 was twice more than in each side at *Re*=2500. The droplets with diameter around 250μm were mostly observed at both *Re* numbers. The probability decreased with increasing the droplet diameter. In addition, there is no great difference of droplets diameter distributions between all sides at both *Re* number.

CONCLUSION

The oil jet behavior ejected from the curved nozzle and the nozzle internal flow distributions were investigated in this research. In addition, the droplets generation process was investigated, and the droplets diameter was measured. The main conclusions from this work are follows.

(1) The oil jet width at all sides (In, Out, Fr, Rr) increased with increasing jet Reynolds number and jet interface began to fluctuate close to the nozzle tip with increasing *Re* number. Droplets were generated from jet interface and ligaments above *Re*=2500.

(2) The mainstream flow velocity of outer side was faster than of inner side in all *Re* numbers. Though the Dean vortex was observed at *Re*=1500, flow from the Out-side to In-side began to appear and flow from In-side to Out-side impinged each other at the center of the nozzle at *Re*=2000, and flow from In-side to Out-side disappeared and Dean vortex was reversed at *Re*=2500. The secondary flow above *Re*=2500 was regarded as the 50% of total droplets at the inner side of the bend.

(3) The 50% of total droplets were generated and droplets diameter around 250μm was mostly observed in the In-side. The difference between the droplets diameter distributions at *Re*=2500 and 3000 was not great but the total number of detected droplets at *Re*=3000 was twice more than at *Re*=2500.

ACKNOWLEDGEMENTS

This investigation was supported by MAZDA Motor Corporation. Oil jet experiment was carried out at fluid engineering laboratory, Hiroshima University.

NOMENCLATURE

Re	oil jet Reynolds number
U	oil jet mean velocity
d	nozzle diameter
v	kinetic viscosity of oil, m^2/s
Fr, Rr, In, Out	the direction of interface
x, y, z	cartesian coordinates, mm
Q	oil jet flow rate
W_m	the area-averaged streamwise velocity
z	the distance from nozzle exit
L	the distance from bend exit

REFERENCES

[1] M. B. Varghese, S. K. Goyal, and A. K. Agarwal. "Numerical and experimental investigation of oil jet cooled piston". *SAE Technical Paper*, pp. 01-1382. 2005.

[2] S.K. Gugulothu, N. Prabhu Kishore, V. Phani Babu, Girish Sapre. "Computational Investigation of Mhd Free Convection on A Flat Vertical Plate Embedded with Micro Polar Fluid". *Acta Mechanica Malaysia*, vol. 2, no. 1, pp. 16-22. 2019.

[3] P. Wang, J. Lv, M. Bai, G. Li, K. Zeng. "The reciprocating motion characteristics of nanofluid inside the piston cooling gallery", *Powder Technology*, Vol. 274, pp. 402-417. 2015.

[4] A. Zada, H. Ullah. "Decomposition Of Cm Through Q-Periodic Discrete Evolution Family". *Matrix Science Mathematic*, vol. 3, no. 1, pp. 09-12. 2019.

[5] K. Sudo, M. Sumida, and H. Hibara. "Experimental investigation on turbulent flow in a circular-sectioned 90-degree bend". *Experiments in Fluids*, Vol. 25, pp. 42-49. 1998.

[6] N. Yaacof, N. Qamaruzzaman, Y. Yusup. "Comparison method of odour impact evaluation using calpuff dispersion modelling and on-site odour monitoring". *Engineering Heritage Journal*, vol. 1, no. 1, pp. 01-05. 2017.

[7] M. Arai, and K. Amagai. "Surface wave transition before breakup on a laminar liquid jet". *International Journal of Heat and Fluid Flow*, Vol. 20, pp. 507-512. 1999.

[8] M. Fayez, M. Mandor, M. El-Hadidy, F. Bendary. "Fuzzy Logic Based Dynamic Braking Scheme for Stabilization of Inter -Area". *Acta Electronica Malaysia*, vol. 3, no. 2, pp. 16-22. 2019.

[9] C. Gong, M. Yang, C. Kang, and Y. Wang. "The acquisition and measurement of surface waves of high-speed liquid jets". *Journal of Visualization*, Vol. 19, pp. 211-224. 2016.

[10] N. Otsu, "A threshold selection method from gray-level histograms", *IEEE-Transactions on Systems Man, and Cybernetics*, Vol. 9, No. 1, pp. 62-66. 1979.

[11] A. Nakashima, G. Nitta, K. Nishida, H. Hongou, H. Yokohata, Y. Ogata. "An experimental investigation of the behaviour of oil jets injected by a 90º curved circular nozzle", *Journal of Fluid Science and Technology*, Vol. 13, No. 1, JFST0007. 2018.